

# OBSERVATION OF SHELL STRUCTURE IN SODIUM NANOWIRES

A.I. Yanson\*, I.K. Yanson\*<sup>†</sup> & J.M. van Ruitenbeek\*

*\*Kamerlingh Onnes Laboratorium,*

*Universiteit Leiden, PO Box 9504, NL-2300 RA Leiden, The Netherlands*

*<sup>†</sup>B. Verkin Institute for Low Temperature Physics and Engineering,*

*National Academy of Sciences, 310164, Kharkiv, Ukraine*

The fact that the rare gas atoms at the end of each row in the periodic table of the elements are exceptionally stable is explained by the closed-shell configuration of their electronic structure. In general, the quantum states of a system of particles in a finite spacial domain form a set of discrete energy eigenvalues, which are usually grouped into bunches of degenerate or close-lying levels, called shells [1]. For fermions this gives rise to a local minimum in the total energy of the system when all states of a given shell are occupied. Shell effects have previously been observed for protons and neutrons in nuclei and for clusters of metal atoms [2–4]. Here, we report the first observation of a shell effect in an open system, a metal nanowire. When recording the statistical distribution of conductance values observed while pulling off the contact between two bulk sodium metal electrodes, the histogram shows oscillations up to contacts larger than 100 atoms in cross section. The period follows the law expected for the electronic shell-closing effect similar to that determining the “magic numbers” in metal clusters [3,4].

Metallic constrictions having the form of nanowires connecting two bulk metal electrodes have recently been studied down to sizes of a single atom in cross section by means of STM and mechanically controllable break-junctions (MCB) [5,6]. By indenting one electrode into another and then pulling them off, a stepwise decrease in electrical conductance is observed, down to the breakpoint when arriving at the last atom. Each scan of the dependence of conductance  $G$  on the elongation  $d$  is individual in details since the atomic configuration of each contact may be widely different. However, statistically, many scans together produce a histogram of the probability for observing a given conductance value, which is quite reproducible for a given metal and for fixed experimental parameters.

A simple description of the electronic properties of metallic nanowires is expected to work best for monovalent free-electron like metals. The alkali metals are most suitable since the bulk electronic states are very well described by free particles in an isotropic homogeneous positive background. In a previous experiment on sodium point contacts [7] a histogram was obtained, which showed pronounced peaks near 1, 3, 5 and 6 times the quantum unit of conductance,  $G_0 = 2e^2/h$ . This is exactly the series of quantum numbers expected for the conductance through an ideal cylindrical conductor. We have now repeated these experiments and extended the range of conductances to much higher values. Although for contacts with a conductance larger than about  $8 G_0$  we do not observe sharp peaks in the histogram centred near multiples of  $G_0$ , we find a number of rather broad peaks, which become stronger and sharper as we increase the sample temperature. We will argue that these arise

from the electronic shell structure of the nanowires.

The MCB technique [6] was adapted for the study of nanowires of the highly reactive alkali metals following Ref. [7] (see Fig 1). Scans were taken continuously by ramping the displacement  $d$  of the electrodes with respect to each other, using the piezo driver. Each individual conductance vs. displacement curve,  $G(d)$ , was recorded in approximately 0.1 seconds from the highest conductance into the tunnelling regime. Histograms of conductance values were accumulated automatically involving  $10^3 - 10^5$  individual scans, and for a number of sample temperatures between 4.2 K and 100 K. Reproducibility and reversibility were verified by periodically returning to the same measuring conditions.

Fig 2 shows the temperature dependence of the histograms for sodium in the range from 0 to  $20 G_0$ . In order to compare different graphs we normalise them by the area. The histograms at low temperatures and low conductances are similar to those observed in Ref. [7]. We clearly recognise the familiar sharp peaks below  $6 G_0$ , while at higher conductances a number of rather wide maxima are found. With increasing temperature we observe a gradual decrease in amplitude of the lower conductance peaks, while the high conductance peaks dramatically sharpen and increase in amplitude. We tentatively attribute this temperature dependence to two mechanisms. First, at low temperatures the nanowires are frozen into the shape, which evolves from mechanical deformations in the breaking and indenting processes. At higher temperature the increased mobility of the atoms allows the system to explore a wider range of atomic configurations and to find the local energy minima. Second, the higher atom mobility may help to remove surface

corrugation leading to the smooth surface required for well-defined electronic shell structure (see below). The decrease in amplitude of the sharp quantization peaks at low conductance can probably be explained by thermally induced breaking of the contact when it consists of only a few atoms.

The central result of this letter is given in Fig 3. The  $T=80$  K sodium histogram up to  $G/G_0 = 120$  is shown in the inset. The smooth background shown by the dashed curve was subtracted, in order to present only the oscillating part, the latter is plotted on a semi-logarithmic scale in the main panel of Fig 3a. Up to 17 oscillations are observed. The positions of maxima are periodic in  $\sqrt{G/G_0}$ , which is proportional to the radius,  $R$ , of the narrowest cross section of the nanowire (see below). This is illustrated in Fig 3b (open squares), where we plot the square root of the positions of the maxima from Fig 3a for consecutively numbered peak index  $i$ , which has the meaning of the shell number. The positions of the peaks reproduce well for about 10 different samples.

In order to explain the periodic peak structure, let us

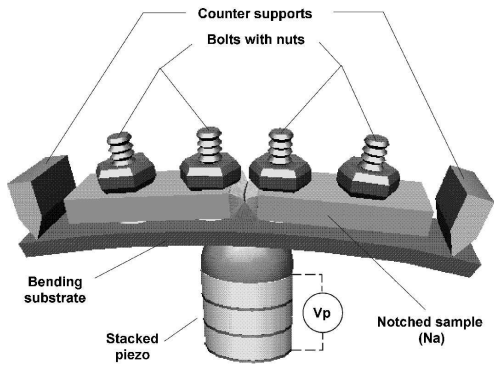


FIG. 1. Schematic view of the MCB technique for alkali metals [7]. While immersed in paraffin oil, the sample is pressed onto four, 1 mm diameter, brass bolts, which are glued onto the isolated substrate. Current and voltage leads are fixed with nuts onto the bolts. A notch is cut into the sample at the centre. This assembly is mounted inside a vacuum can, which is immersed in liquid helium. By bending the substrate at 4.2 K in vacuum, the sample is broken at the notch. Two fresh surfaces are exposed, and their distance is adjusted by changing the force on the substrate, employing a piezo element for fine control. The temperature of the sample is controlled by a heater and thermometer, which are fixed at the bottom of the substrate. The cryo-pumping action of the low temperature environment ensures that the surfaces are not polluted by adsorbates. The purity of the sodium metal was at least 99.9%. The conductance was recorded using a standard DC-voltage bias 4 terminal technique, measuring the current with 16-bit resolution. The drift and calibration of the current-to-voltage converter was verified against standard resistors corresponding to 1, 10 and 100  $G_0$ , leading to an overall accuracy in the conductance better than 1% for  $G > 10G_0$ .

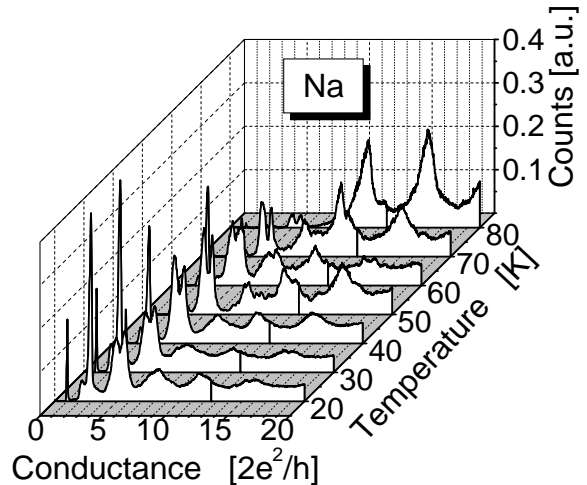


FIG. 2. Temperature evolution of sodium histograms in the range from 0 to 20  $G_0$ . The voltage bias was 10 mV and each histogram is constructed from 1000-2000 individual scans. The amplitude has been normalised by the total area under each histogram.

first remind the very general relations held for any solution of wave equations in a finite domain [1]. Fluctuations in the density of energy levels at the Fermi energy  $\delta\rho_F$  as a function of system size give rise to fluctuations in the free energy of the system [4]. The periods of oscillation correspond to quasi-classical closed orbits described inside the domain, where the allowed orbits obey the Bohr-Sommerfeld quantization condition  $\oint pdq = \hbar k_F L = n\hbar$  ( $n = 1, 2, 3, \dots$ ), which is equivalent to demanding that the path length  $L$  be an integer multiple of the Fermi wavelength  $\lambda_F = 2\pi/k_F$ . For spherical metal clusters, the dominant periods arise from only two such paths, which are called the stationary paths in the periodic orbital theory [1,4], namely the three and four vertices polygons (triangles and squares) inscribed into the diametrical cross section of the sphere (see the insets in Fig 4, with indices (3.1) and (4.1)).

The fluctuations in the density of states for a free electron nanowire and their influence on the free energy of the system was recently considered in a number of theoretical papers [8–13]. H"oppler and Zwerger [13] give the semi-classical Balian-Bloch expression for these fluctuations for a cylindrical nanowire with a circular cross section and a square hard-wall potential, and compare the results to an exact calculation for the same model system. They show that a semi-classical shell model with only the lowest three orbits included (line, triangle and square, see inset Fig. 4) gives a good description of the main features. We use this approximation, and their expression for the fluctuating part of the free energy in terms of the density of states [8,13], to calculate the positions of the local energy minima as a function of the wire radius for this model. In order to compare with Fig 3, the smooth back-

ground of the energy was subtracted in the same manner as for the histogram in Fig 3a, leaving the oscillatory part to be positive. The ordinate axis is again logarithmic, and at the minima in the free energy one expects to observe a maximum in the stability of the nanowire. The conductance corresponding to a given wire radius can be estimated using the semi-classical expression for a ballistic wire [14],

$$G/G_0 \simeq \left(\frac{\pi R}{\lambda_F}\right)^2 \left(1 - \frac{\lambda_F}{\pi R}\right). \quad (1)$$

The positions of the energy minima are plotted as a function of shell number in Fig 3b (open triangles), while

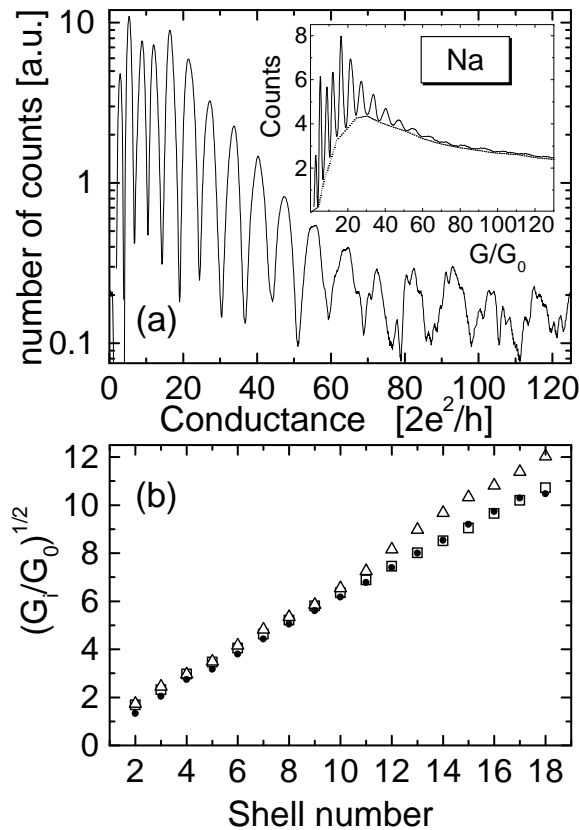


FIG. 3. (a) Histogram of the number of times each conductance is observed versus the conductance in units of the conductance quantum,  $G_0$ , for sodium at  $T=80$  K and bias voltage  $V=100$  mV, constructed from over 10,000 individual scans. The inset shows the raw data and the smooth background (dashed curve), which is subtracted in the main graph. The logarithmic scale for ordinate axis helps to display the smaller amplitude features at high conductance values. (b) Square root of the positions of the maxima in (a),  $\sqrt{G_i/G_0}$ , versus shell number (open squares). The experimental peak positions are compared to the expected positions derived from the magic numbers of metallic clusters (filled circles) and to those expected from a semi-classical description for the fluctuations in the free energy for the nanowire (open triangles).

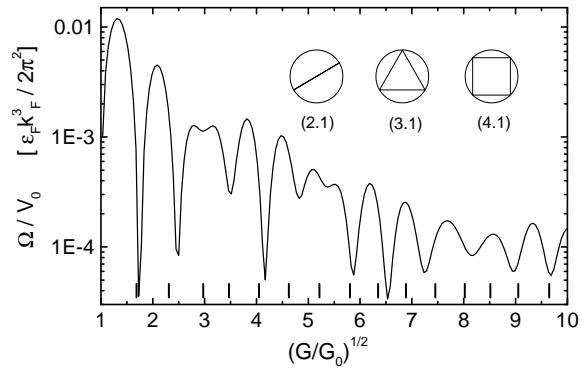


FIG. 4. The fluctuating part of the thermodynamic potential,  $\Omega$ , per volume of the wire,  $V_0$ , versus the square root of the conductance for sodium nanowires (taking  $E_F = 2.8$  eV), after Ref. [13]. Note the logarithmic scale for the ordinate axis. Vertical bars near the abscissa denote the positions of maxima in conductance histogram of Fig 3a.

The insets show three semi-classical quantization trajectories, i.e. diametrical, triangular and square closed paths, where the indices  $(v.w)$  give the number of vertices,  $v$  and the winding number,  $w$ .

the positions of the experimental peaks are indicated by bars at the bottom of Fig 4. The gross behaviour of the oscillations in Figs 3a and 4 is similar, namely: *i*) the majority of oscillation periods approximately coincide with each other, *ii*) the slope of theoretical curve at  $i \leq 9$  and  $i \geq 14$  coincides with the experimental one ( $\Delta\sqrt{G_i/G_0} = 0.57 \pm 0.01$ ), and *iii*) the amplitudes of the oscillations drop by about two orders of magnitude. However, there is difference in details: *i*) the calculated minima at  $\sqrt{G/G_0} \simeq 3$  and  $5.3$  are shallow, while in the experimental histogram the peak amplitudes monotonously decrease, and *ii*) the theoretical curve has a kink due to interference of the three stationary path contributions, which is not resolved in the experiment.

Our interpretation uses the approximately linear semi-classical relation between conductance and wire cross section, Eq. (1). Corrections may arise from two mechanisms. First, back scattering on defects (or phonons) may shift the peak positions. Both the fact that strong scattering would tend to smear the peak structure and the close agreement between the experimental and theoretical periodicity, suggest that this shift is small. Second, the mechanism of level-bunching leading to fluctuations in the free energy should also give rise to fluctuation corrections to Eq. (1), which by itself would lead to peaks in the histograms even for a perfectly smooth distribution of wire diameters. Peaks due to this mechanism would be found at those points where the increase of the conductance with wire diameter is slow. Thus the two mechanisms (fluctuations in the free energy and fluctuations in the conductance as a function of wire radius) lead to the same periodic peak structure. The two phe-

nomena are likely to co-operate, possibly explaining why the shell effect is so clearly pronounced.

Alternatively, we may compare our experimental results directly with the experimental cluster magic numbers. This should be possible since the same stationary paths determine the energy fluctuations for clusters [4] as for nanowires [13]. Some deviations may arise from differences in phase and relative amplitude for each of the three geometrical paths for clusters and wires. The radius of the clusters is obtained from the number of atoms,  $N$ , in the cluster using [3,4]  $R = r_s N^{1/3}$ , with  $r_s$  the Wigner-Seitz radius of an atom. For the nanowires we obtain the conductance corresponding to this radius through Eq. (1). In Fig 3b (filled circles) we show the accordingly calculated peak positions, where the cluster magic numbers  $N_i$  were taken from the experimental mass abundance spectra [3]. We establish a direct correspondence between preferential values for the conductance in histograms for sodium nanowires, and the magic numbers  $N_i$  observed in cluster abundance spectra.

- [11] Yannouleas, C. & Landman, U., On mesoscopic forces and quantized conductance in model metallic nanowires. *J. Phys. Chem. B* **101**, 5780-5783 (1997).
- [12] Yannouleas, C., Bogachek, E.N. & Landman, U. Energetics, forces, and quantized conductance in jellium-modeled metallic nanowires. *Phys. Rev. B* **57**, 4872-4882 (1998).
- [13] Höppler, C. & Zwerger, W. Quantum fluctuations in the cohesive force of metallic nanowires, *preprint, cond-mat/9810134*.
- [14] Torres, J.A., Pascual, J.I. & Sáenz, J.J. Theory of conduction through narrow constrictions in a three-dimensional electron gas, *Phys. Rev. B* **49**, 16581-16584 (1994).

**Acknowledgements.** We thank L.J. de Jongh for his continuous support.

- 
- [1] Balian, R. & Bloch, C. Distribution of eigenfrequencies for the wave equation in a finite domain: III. Eigenfrequency density oscillations. *Ann. Phys.(N.Y.)* **69**, 76-160 (1972).
  - [2] Bohr, Å. & Mottelson, B.R. *Nuclear Structure*, Vol.II (Benjamin, Reading, MA, 1975).
  - [3] de Heer, W.A. The physics of simple metal cluster: experimental aspects and simple models. *Rev. Mod. Phys.* **65**, 611-676 (1993).
  - [4] Brack, M. The physics of simple metal clusters: self-consistent jellium model and semiclassical approaches. *Rev. Mod. Phys.* **65**, 677-732 (1993).
  - [5] Agraït, N., Rodrigo, J.G. & Vieira, S. Conductance steps and quantization in atomic-size contacts. *Phys. Rev. B* **47**, 12345-12348 (1993).
  - [6] Muller, C.J., van Ruitenbeek, J.M., & de Jongh, L.J. Experimental observation of the transition from weak link to tunnel junction. *Physica C* **191**, 485-504 (1992).
  - [7] Krans, J.M., van Ruitenbeek, J.M., Fisun, V.V., Yanson, I.K. & de Jongh, L.J. The signature of conductance quantization in metallic point contacts. *Nature* **375**, 767-769 (1995).
  - [8] Stafford, C.A., Baeriswyl, D. & Bürki, J. Jellium model of metallic nanocoherence. *Phys. Rev. Lett.* **79**, 2863-2866 (1997).
  - [9] Kassubek, F., Stafford, C.A. & Grabert, H. Force, charge, and conductance of an ideal metallic nanowire, *preprint, cond-mat/9809318*.
  - [10] van Ruitenbeek, J.M., Devoret, M.H., Esteve, D. & Urbina, C. Conductance quantization in metals: The influence of subband formation on the relative stability of specific contact diameters. *Phys. Rev. B* **56**, 12566-12572 (1997).